Indian Journal of Chemical Technology
Vol. 24, May 2017, pp. 239-255

Response surface methodology for optimization of phenol adsorption by activated carbon: Isotherm and kinetics study

Dorra Tabassi*, Soumaya Harbi, Islem Louati & Bechir Hamrouni

Desalination and Water Treatment Research Unit,
Faculty of Science of Tunis, University of Tunis El Manar, 2092 manar II, Tunisia
E-mail: dorratabassi@gmail.com

Received 1 October 2015; accepted 3 June 2016

The effect of four different parameters such as *p*H, initial phenol concentration, adsorbent dose and temperature on the adsorptive removal of phenol from aqueous solution over commercial granular activated carbon (GAC) has been studied. Two-level full factorial design (FFD) combined with response surface methodology (RSM) have applied to find the best operating conditions. The optimum *p*H, initial phenol concentration, adsorbent dose and temperature have been found by applying desirability function (DF) to be 6, 1000 mg/L, 3 g and 28.75°C. The granular activated carbon has been characterized using different physicochemical methods. The experimental data best fits in Freundlich isotherm Equation and the removal follow pseudo-first-order kinetics. Thermodynamic parameter reveals that the removal process is feasible, exothermic and spontaneous in nature. The adsorbent is regenerated with 0.1 M NaOH solution for further reuse.

Keywords: Activated carbon, Adsorption, Phenol, Response surface methodology, Two-level full factorial design

Industrial processes generate a variety of molecules that may pollute waters due to negative impacts of ecosystems and humans (toxicity, carcinogenic and mutagenic properties). Hence, the treatment of effluents containing toxic compounds has been one of the main important fields of studies. Phenols are one of the commonly known chemical products used in various aqueous industrial wastes and they are among the most prevalent forms of chemical pollutants in the industrial wastewater of oil refineries, petrochemical plants, ceramic plants, coal conversion processes, phenolic resin industries and pharmaceutical industries[1-4]. It has been listed as priority pollutant by the Agency for Toxic Substances and Disease Registry (ATSDR)[5]. The World Health Organization (WHO) fixed the permissible concentration of phenolic contents in potable water at 1 μg/L and the regulations by the Environmental Protection Agency (EPA), call for lowering phenol content in wastewaters less than 1 mg/L[6,7]. Phenol is reported to be associated with intense acute and chronic toxic effect on human health such as headache, vomiting, liver and kidney damage, fainting and other mental disorders. Considering the environmental implications, removal of phenol is important for safe discharge. Therefore, several methods for the treatment of phenolic wastewater have been proposed in the literature. These include biological degradation[8], chemical oxidation[9], solvent extraction[10], separation with membrane process[11,12] and adsorption. Compared to other methods, adsorption technique is widely used for water treatment due to its sludge free clean operation, economical, availability of wide range of adsorbents and complete removal of phenols from wastewaters. The most usual adsorbents for water treatment are activated carbons due to the carbon's high specific surface area, ample pore size and reasonably high mechanical strength[13,14]. Activated carbon was studied as a phenol sorbent either at fixed conditions or by considering the effect of some important parameters such as contact time, adsorbent dose, solution *p*H, temperature, phenol concentration and ionic strength[15,16].

Traditional research methods generally study the effect of one variable at a time, because it is statistically easier to manipulate. However, in many cases, two factors may be interdependent, and it is impractical or false to analyze them in the traditional way. But the studying of each and every factor is quite tedious and time consuming. These limitations of classical methods can be eliminated by optimizing all the affecting parameters collectively by statistical experimental design such as response surface methodology (RSM). RSM, initially described by Box and Wilson[17], is a collection of mathematical and statistical techniques useful for the modeling and analysis of problems in which a response of interest is influenced by several variables and the objective is to optimize this response[18]. In literature, RSM based on two-level full factorial design (FFD) has been used in adsorption process such as the adsorption of Cr (VI) on activated carbon[19], the adsorption of brilliant yellow dye adsorption onto sepiolite[20], and more.

The intention of the present research is the investigation of adsorption and desorption of phenol onto GAC. Adsorption parameters such as adsorbent dose, initial *p*H, initial phenol concentration and temperature on phenol removal were analyzed and optimized using the FFD combined with RSM and the desirability function. The adsorbent was characterized by SEM, BET, Fourier Transform Infrared spectra (FTIR), X-ray diffraction, Boehm titration and determination of $p\text{H}_{\text{pzc}}$. The kinetic and thermodynamic parameters were calculated to determine the adsorption mechanism. The adsorption equilibrium was evaluated by fitting the experimental data to isotherm model such as Langmuir, Freundlich, Temkin, Dubinin-Radushkevich and Redlich-Peterson models. Kinetic data obtained from the batch adsorption studies were fitted to pseudo-first order, pseudo-second order and intraparticle diffusion model.

Experimental Section

Adsorbent

The GAC (NORIT 1240) used in this study was purchased from Sigma Aldrich. Prior to use, the carbon was pretreated by boiling in ultra-high quality (UHQ) water for 1 h and washed repeatedly with UHQ water. Finally, the washed activated carbon was dried in an oven at 110°C to constant weight and stored in desiccators until use. The various physic-chemical characteristics of the GAC were given in Table 1.

Characterization of activated carbon

Structural characterization of the GAC was done using N_2 adsorption isotherm at 77K using an ASAP 2020 Micromeritics instrument. Prior to gas adsorption measurement, the activated carbon was degassed in vacuum at 100°C for at least 6 h. The specific surface areas (S_{BET}) were calculated using the Brunauer-Emmett-Teller (BET) method. Pore distribution was determinate using the Barrett-Joyner-Halenda (BJH) methods[21]. The t-plot method was applied to calculate the micropore volume and the mesopore volume was determined by substracting the micropore volume from total pore volume. Scanning electron microscopic (SEM) (JEOL JSM 5400) analysis was carried out for the activated carbon to study the surface morphology and to verify the porosity. The crystalline structure of GAC was determined via X-ray diffractiometer (Panalytical model X'pert PRO MPD).

Table 1—Physico-chemical characteristics of the GAC

Parameters	Values
Bulk density(g/cm^3)	0,5
Particle size (mm)	0,6 - 0,7
Moisture (%)	< 5
Ash (%)	12

Surface functional groups were determined by standard neutralization-titration with HCl, NaOH, Na_2CO_3, $NaHCO_3$ (0.05M in water) according to the Boehm procedure[22]. The number and type of acid groups were calculated by considering that the difference between NaOH and Na_2CO_3 consumption corresponds to the weakly acidic phenolic groups, while difference between Na_2CO_3 and $NaHCO_3$ consumption corresponds to the lactonic groups. Carboxylic groups were therefore quantified by direct titration with $NaHCO_3$. On the other hand, total basic sites were evaluated by titration with HCl. The results of Boehm titration were supported by FTIR.

The *p*H of the point of zero charge ($p\text{H}_{\text{PZC}}$), i.e. the *p*H above which the total surface of the carbon particles is negatively charged, was measured by the so-called *p*H drift method[23]. Accurately weighed portions of each carbon (0.1g) were filled into 50 mL conical flasks containing 25 mL of 0.1M NaCl standard solutions. The initial *p*H's of these solutions were varied (*p*H 2-12) and then shaken mechanically for 48 h. Initial *p*H was adjusted by adding either HCl or NaOH (0.2M). After a period of 48 h shaking, the final *p*H values of the suspensions were determined using a *p*H-meter. The final *p*H values were plotted against the initial *p*H values and the *p*H at which the curve crosses the line *p*H (final) = *p*H (initial) is taken as the $p\text{H}_{\text{pzc}}$ of the given carbon.

Adsorbate

Phenol (C_6H_5OH) of analytical reagent (AR) grade supplied by FLUKA was used for the preparation of the synthetic adsorbate solutions of various C_0 in the range of 10-2000 mg/L. The required quantity of phenol was accurately weighed and dissolved in a small amount of distilled water and subsequently made-up to 1L in a measuring flask. Fresh stock solution as required was prepared every day and was stored in a brown color glass reservoir to prevent photo-oxidation.

Batch adsorption studies

The batch experiments were carried for the optimization process according to the FFD. For this, 100 mL of phenol aqueous solution with different *p*H, initial phenol concentration, temperature, and adsorbent dose was taken in 200 mL Erlenmeyer flasks. Initial *p*H of the solution was adjusted with 0.1M HCl and NaOH using *p*H meter. The mixture was agitated in a temperature controlled water bath shaker (Grant OLS 200) at fixed contact time (120 min) that was obtained from kinetic study and at a constant agitation speed of 130 rpm to achieve equilibrium. After equilibrium, the solutions were filtered and the concentration of the phenol in the solution was determined measured by the Standard Methods using potassium ferricyanide and 4-aminoantipyrine[24] and analyzed by a spectrophotometer (TOMOS V-1100) at 510 nm. The extent adsorption of phenol in percentage was calculated by using following Equation:

$$\%\mathrm{R} = \left(\frac{\mathrm{C_i}-\mathrm{C_t}}{\mathrm{C_i}}\right) \times 100 \qquad \dots (1)$$

where C_i and C_t are the phenol concentrations in mg/L initially and at a given time t respectively. The phenol adsorption capacities were determined by using the Equation:

$$\mathrm{q_e} = \frac{(\mathrm{C_i}-\mathrm{C_e})\times \mathrm{V}}{\mathrm{m}} \qquad \dots (2)$$

where V is the volume of phenol solutions (L), C_i is the initial concentration (mg/L), C_e is the equilibrium concentration (mg/L), and m is the mass of the adsorbent (g).

Kinetic studies were conducted at four different concentrations (10, 50 and 500 mg/L) of the phenols at 25°C, solution *p*H was not adjusted. Samples were withdrawn at regular intervals to plot the amount adsorbed versus time. Isotherm experiments were performed using different initial concentrations ranging between 10 and 2000 mg/L at different temperature.

Validation of analytical method

In order for the method to be used in laboratories as a routine analysis procedure, performance criteria were examined for parameters including linearity, sensitivity, specificity, fidelity (repeatability and reproducibility) and instrumental method detection and quantification. The validation of the analytical method for determining residual phenol concentration by 4-aminoantipyrine was performed according to the French standard XPT-90-210. The results are shown in Table 2.

As shown in Table 2, the method exhibited good linearity, high precision, high sensitivity, and suitable selectivity and specificity over a range of concentrations of 0.5 to 5 mg/L with a detection limit of 0.02 mg/L and a quantification limit of 0.066 mg/L.

Desorption and regeneration studies

The recycling of sorbent is a most important aspect from the economical point. After adsorption, the phenol loaded carbon was washed with distilled water to remove the unabsorbed adsorbate. Several such carbon samples were prepared. The loaded carbon was resuspended in 50 mL of 0.001, 0.005, 0.1, 0.15 and 0.2 M NaOH and was equilibrated for 2 h. It was centrifuged and the concentration of phenol in supernatant solution was determined as described above. The percentage desorption from the spent

Table 2—Results of validation of the analytical method

Test	Experimental value	Critic value	Conclusion
Linearity	F_l=2794.266 F_{nl}=0.472	V_{Cl}= 7.82 V_{Cnl}=4.22	The method is linear. No curvature or The linearity is approved
Specificity	t_{obs}=0.740 t'_{obs}=0.274	$t_{(8,0.995)}$=3.355	Slope equal to 1. Origin intercept is equal to 0 and the method is specific
Cochran	C_{xobs}=0.421	$C_{cochran,\alpha=5\%=}$0.480 $C_{cochran,\alpha=1\%}$= 0.564	Point group is considered no aberrant Point group is considered no suspect
Fidelity	CV_r=2.410% ;1.550% ; 0.473% ;3.821%	CV_r<5%	Repeatable faithful
	CV_R=0.459%	CV_R<5%	The method is reproducible

adsorbent was calculated from the amount of phenol adsorbed on activated carbon and the final concentration of phenol in the desorption medium.

Experimental design

The objective of RSM is to optimize a response which is influenced by several independent input factors by understanding their interactions and their effects on response. The RSM was widely applied in chemical engineering and sorption process optimization. The various techniques used in RSM are Central Composite Design (CCD), Box-Behnken statistical experiment design (BBD) and two-level full factorial design (FFD).

The FFD with only two values (levels) for all design variables are the most frequently used designs. This is mainly due to the following facts: *i*) the number of experiments is less than with more levels, and *ii*) the results can be analyzed using regression analysis for both qualitative and quantitative variables. A FFD is often used by scientists wishing to understand the effect of two or more independent variables upon a single dependent variable. A common experimental design is one with all input factors set at two-levels each. These levels are called 'high' and 'low' or '+1' and '−1' respectively. If there are k factors each at two- levels, a FFD has 2^k runs.

In the present study, four factors (X1, X2, X3, X4) and two level (-1, +1) was set. The total number of experiments results from applied plan of 2^4 types is 16. The relation between desired response and independent variables can be written as:

$$Y = f(X1X2X3X4) \quad \ldots (3)$$

In order to get true functional relationship between independent variables and the response, a polynomial equation was used to describe the effect of on response.

$$Y = b_0 + b_1 X1 + b_2 X2 + b_3 X3 + b_4 X4 + b_{12} X1X2 + b_{13} X1X3 + b_{14} X1X14 + b_{23} X2X3 + b_{24} X2X4 + b_{34} X3X4 + b_{123} X1X2X3 + b_{124} X1X2X4 + b_{134} X1X3X4 + b_{234} X2X3X4 + b_{1234} X1X2X3X4 \quad \ldots (4)$$

The regression coefficients are computed as below

$$b_0 = \sum \frac{Y}{N} \quad \ldots (5)$$

$$b_i = \sum \frac{X_i Y}{N} \quad \ldots (6)$$

$$b_{ni} = \sum \frac{(X_{ni} X_i) Y}{N} \quad \ldots (7)$$

where X_i are values indicate the corresponding parameters in their coded forms;

b_0 is the average value of the result,
b_1, b_2, b_3 and b_4 are the linear coefficients,
b_{12},b_{13} ,b_{14} ,b_{23} ,b_{24} ,b_{34} ,b_{123} ,b_{124} ,b_{134},b_{234} ,b_{1234} represent the interaction coefficients,

N is the number of total experiments conducted. Experimental data were analyzed using STATISTCA, a statistical software package version 12.0., and fitted to a second-order polynomial model. This software was used for regression analysis of the data obtained and to estimate the coefficient of regression equation. The statistical significance of the model was justified through analysis of variance (ANOVA) for polynomial model with 95% confidence level, and residual plots were used to examine the goodness of models fit. The quality of the polynomial model was expressed by the coefficient of determination, namely, R^2 and Adj-R^2. The surface of response were developed using the same program. Also, the optimum values of factors were determinate using a target in the program (response desirability profiling).

Results and Discussion

Characterization of the activated carbon

The pH_{pzc} was determined from Fig. 1. The pH_{pzc} is the point were the curve pH_f vs pH_i intersects the line pH_i=pH_f. The pH_{pzc} was found to be 7.2, at which the net surface charge on GAC was zero. At $pH < pH_{pzc}$, the GAC surface had a net positive charge, while at $pH > pH_{pzc}$ the surface had a net negative charge.

According to the results of the Boehm titration (Table 3), the difference between the total number of the surface basic sites and the total number of the surface acid sites is low. This is in agreement with pH_{pzc}, which is also neutral.

While quantitative analysis of the surface chemistry was given by Boehm titration and pH_{pzc}, a

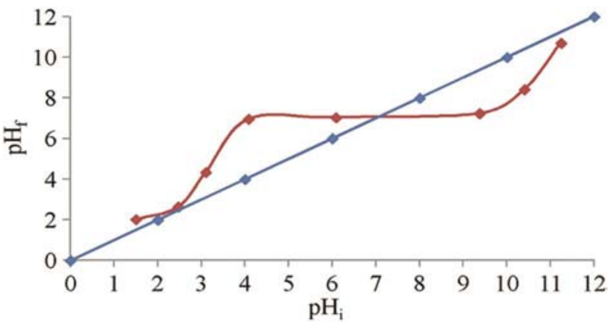

Fig. 1 — *p*H titration of GAC

Table 3 — Concentration of surface functional groups on GAC samples

Functions	Carboxylic	Lactone	Phenolic	Total acidity	Total basicity
Quantity (mmol/g)	0,06	0,04	0,04	0,14	0,2

qualitative analysis of activated carbon can be carried out by FTIR spectrum.

The spectra of the granular activated carbon and adsorbed phenol activated carbon were measured by an FTIR spectrometer within the range of 400-4000 cm^{-1} wave number. The FTIR spectrum plot was obtained for the granular activated carbon and adsorbed phenol activated carbon. The presence of absorption band at 3441.6 cm^{-1} can be attributed to the O–H stretching vibrations of hydrogen bonded hydroxyl groups. The very weak peak at 2842.1 cm^{-1} is attributed to the aliphatic C–H stretching vibration. The band around 1679.6 cm^{-1} can be ascribed to C=O stretching vibrations of ketones, aldehydes, lactones or carboxyl groups. The aliphatic C–H bending vibration occurs at 1460 cm^{-1}. The band located around 1075 cm^{-1} is typically attributed to C–O groups of carboxylic acid. The region between 700 and 900 cm^{-1} contains various bands related to the aromatics, out of plane C–H bending with different degrees of substitution[25]. After adsorption of phenol, the peaks of the C–H bending vibration gets shifted to a lower frequency at 1398 cm^{-1}, and the aromatic C–O groups of carboxylic acid disappears completely. This disappearance of this peak indicates that the alkyl and aromatic C–O functional groups of GAC coordinate with phenol by Van der Waals forces. In addition the presence of a wide band located at 3427.9 cm^{-1} which is typically attributed to hydroxyl groups stretching vibrations, another band in 1089.2 cm^{-1} caused by the stretching vibration of C–O, all are FTIR characteristics of phenol. The results confirmed that the phenol has been successfully adsorbed by the GAC.

Activated carbon can be crystallographically characterized by means of X-ray diffraction (XRD). XRD spectrum for granular activated carbon is given in Fig. 2. The peaks where located at $2\theta = 20.9, 26.7, 42.4, \text{and } 50.2$ for akdalaite [(Al_2O_3) $4H_2O$)], moganite (SiO_2), tamarguite [NaAl $(SO_4)_2 6H_2O$] and Fersilicate (FeSi)[26], respectively, which are major components present in GAC . The broad peak in the XRD indicates the presence of amorphous form of silica. Any diffracted peak due to crystalline carbon was not observed in the XRD pattern. A similar result was found by Suresh *et al.*[27] and Rameshrajaa *et al.*[26]

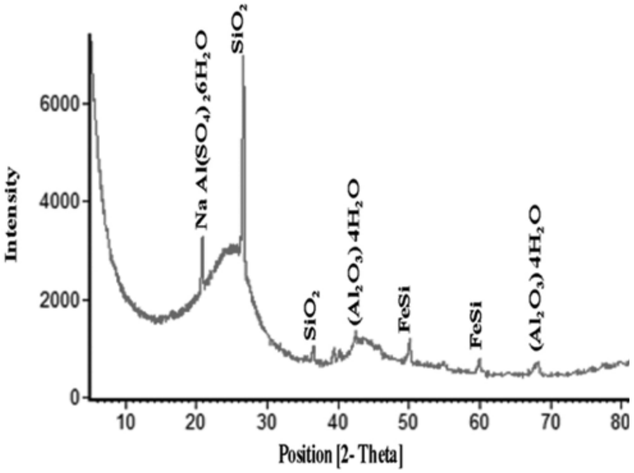

Fig. 2 — XRD pattern of GAC

The adsorption isotherms of N_2 on GAC were obtained. The shape of the N_2 adsorption isotherms for the carbon is of type II based on IUPAC classification[28], which is a characteristic of simultaneous presence of microspores and mesopores. The BET surface area (S_{BET}), external surface area (S_{ext}), micropore surface area (S_{mic}), total pore volume (V_{tot}), micropore volume (V_{mic}), mesopore volume (V_{mes}) and average pore diameter for the activated carbon are listed in Table 4. The BET surface area of the activated carbon is 866.32 m^2/g. Total pore volume is 0.451 cm^3/g and mesopore volume is 0.277 cm^3/g, indicating that the activated carbon contain mostly mesopores. The analysis of the BJH pore distribution of GAC shows that the micropores (d<20 Å) occupy about 38.6% of the total pore volume and the mesopores account for about 61.4% of the total pore volume. The average pore diameter of GAC was found to be 29.45 Å. In accordance with the IUPAC classification, the GAC exhibits mesoporous nature (20 Å < average pore diameter < 500 Å), which is desirable for the liquid phase adsorption of organic compounds.

The morphology of GAC was examined under Scanning electron microscope (SEM). The SEMs of the blank GAC and phenol loaded GAC are shown in Fig. 3. SEM shows that the GAC is crystalline in nature and with varying particle size. The presence of various sizes of pore and a large surface area make the adsorbent suitable to adsorb a wide variety of species.

Table 4 — Porous structure parameters of GAC

S_{BET} (m^2/g)	S_{ext}(m^2/g)	S_{mic}(m^2/g)	V_{tot} (cm^3/g)	V_{mic}(cm^3/g)	V_{mes}(cm^3/g)	Pore diameter (Å)
866.32	474.11	392.21	0.451	0.174	0.277	29.45

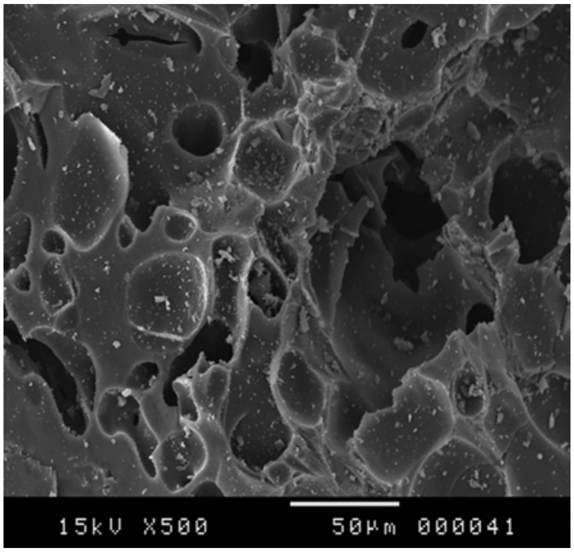

Fig. 3 — SEM image of GAC

Two level full factorial design statistical analysis

usually depends on several factors. These are initial phenol concentration, acidity of medium (*p*H), time of contact between the adsorbent and the sorbent, the adsorbent dosage and temperature.

In this study, the combined effect of initial *p*H, initial concentration, adsorbent dose and temperature has been investigated by using full factorial design. The results of the experimental design were analyzed using STATISTICA 12 software to evaluate the effects as well as the statistical parameters, the statistical plots (Pareto, normal probability of the standardized effect, main effect and surface plot).

Table 5 presents a ranges of the four studied process parameters (X1 – *p*H, X2– initial concentration of phenol (Ci), X3 – adsorbent dose (m) and X4 – temperature (T) and their levels of independent reactions conditions (-1 and +1).

The design matrix consisting in 16 sets of experimental conditions in coded values for factors along with their values for the responses (% removal efficiency) are given in Table 6. The phenol removal efficiency was found between 28.57 % and 99.22 %.

The following codified equation was used to explain the 2^4 factorial designs were:

$$Y = b_0 + b_1 X1 + b_2 X2 + b_3 X3 + b_4 X4 + b_{12} X1X2 + b_{13} X1X3 + b_{14} X1X4 + b_{23} X2X3 + b_{24} X2X4 + b_{34} X3X4 + b_{123} X1X2X3 + b_{124} X1X2X4 + b_{134} X1X3X4 + b_{234} X2X3X4 + b_{1234} X1X2X3X4 \quad \ldots (8)$$

where R (%) is the percentage removal of phenol, b_0 is the global mean; b_i represents the regression coefficient relating to the main factor effect and interactions, and X_1, X_2, X_3 and X_4 stand for *p*H, initial concentration, adsorbent dose and temperature, respectively. The main and interaction effects, coefficients of the model and standard errors were shown in Table 7.

The X1X2X3, X1X2X4, X1X3X4, X2X3X4, X1X2X3X4 effects were insignificant, when it was compared with other effects. Thus these effects were neglected and did not include in the model equation. Substituting the coefficients b_i in Eq (8), by the respective value from Table 7, we get:

$$Y = 73.283 - 8.206X1 - 7.709X2 + 14.777X3 - 4.524X4 - 4.603X1X2 + 1.164X1X3 + 6.321X2X3 - 0.658X1X4 - 0.347X2X4 - 0.334X3X4 \quad \ldots (9)$$

The main effects (X1, X2, X3 and X4) symbolize deviations of the R(%) between high and low level for each one of them (Fig. 4). It is clear that the variables considered for this investigation play an important role in the adsorption of phenol removal since each variable has a significant contribution on the percentage of phenol removal.

A change in the level of X1, X3 and X4 from min to max results in 16.41%, 15.41% and 9.04% decrease in the R (%), respectively. The *p*H, initial concentration and temperature have a negative effect on the percentage of adsorption of phenol. Thus, upon changing the level of X2 from low to high level, the R (%) is amplified by 29.55%. Consequently adsorbent dose had a positive effect.

Student's test

Student's test value revealed that terms of adsorbent dose (t= 8.93) imposed the greatest effect on the removal efficiency of phenol in the studied range. Also the *p*H (t = - 4.96) and initial concentration (t = - 4.65) has a significant effect on the removal efficiency of phenol. The analysis also indicated that the X2X3interaction (t = 3.82), X1X2

Table 5 — Process variables and their level for the adsorption of phenol by FFD

Factors	Name	Units	Low actual	High actual	Low code	High code
X1	pH	-	6	10	-1	+1
X2	Initial concentration	mg/ L	50	1000	-1	+1
X3	Adsorbent dose	g	0.5	3	-1	+1
X4	Temperature	°C	25	40	-1	+1

Table 6—Experimental design in term of coded factors and results of the FFD

Run no.	Coded values Independent variables				Y(%)	
	X_1	X_2	X_3	X_4	Observed	Predicted
1	-1	-1	-1	-1	80.19	80.84
2	+1	-1	-1	-1	75.36	72.16
3	-1	+1	-1	-1	66.66	62.32
4	+1	+1	-1	-1	28.57	35.69
5	-1	-1	+1	-1	95.35	95.74
6	+1	-1	+1	-1	89.77	92.17
7	-1	+1	+1	-1	99.22	102.86
8	+1	+1	+1	-1	87.33	80.89
9	-1	-1	-1	+1	72.98	74.11
10	+1	-1	-1	+1	61.61	63.26
11	-1	+1	-1	+1	51.67	54.56
12	+1	+1	-1	+1	31.00	25.30
13	-1	-1	+1	+1	89.86	88.03
14	+1	-1	+1	+1	82.81	81.84
15	-1	+1	+1	+1	95.98	93.77
16	+1	+1	+1	+1	64.16	69.16

Table 7—Statistical parameters for 2^4 designs

Term	Effect	Coefficient	Standard error coefficient
b_0		73.28	1.6544
b_1	-16.41	-8.20	1.6544
b_2	-15.41	-7.70	1.6544
b_3	29.55	14.77	1.6544
b_4	-9.04	-4.52	1.6544
b_1b_2	-9.20	-4.60	1.6544
b_1b_3	2.32	1.16	1.6544
b_1b_4	-1.31	-0.65	1.6544
b_2b_3	12.64	6.32	1.6544
b_2b_4	-0.69	-0.34	1.6544
b_3b_4	-0.66	-0.33	1.6544

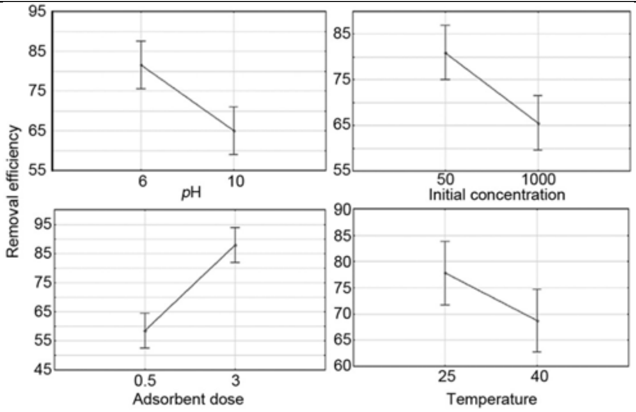

Fig. 4 — Plots of main effects

interaction (t = - 2.78), temperature (t = - 2.73) had a marked effects. All other interactions were found insignificant. Figure 5a presents the Pareto chart which is a series of bars whose heights reflect the frequency or impact of parameter. The bars are arranged in descending order of height from left to right. To indicate the minimum statistically significant effect, a vertical line, which located at a critical value of Student's (p=0.05), is drawn in the Pareto chart (Fig. 5b). This means the factors represented by the bars to the right of the reference line in the Pareto chart, are relatively more significant. Analysis revealed that all main factors, X1X2 and X2X3 interactions effect were significant at a 5% probability level (p <0.005) while the interaction effect X1X3, X1X4, X2X4 and X3X4 were not significant, since it presented a probability value higher than 0.05.

Analysis of variance (ANOVA)

Determination of the significant main and interaction effects of factors affecting the removal efficiency of phenol was followed by performing an analysis of variance (ANOVA) given in Table 8. The sun of squares (SS) and the mean square (MS) of each factor, p value (defined as the level of significance to the rejection of the null hypothesis) and the F-value (defined as the ratio of mean square effect and the mean square error) were also represented. For 95% confidence level, 1 degree of

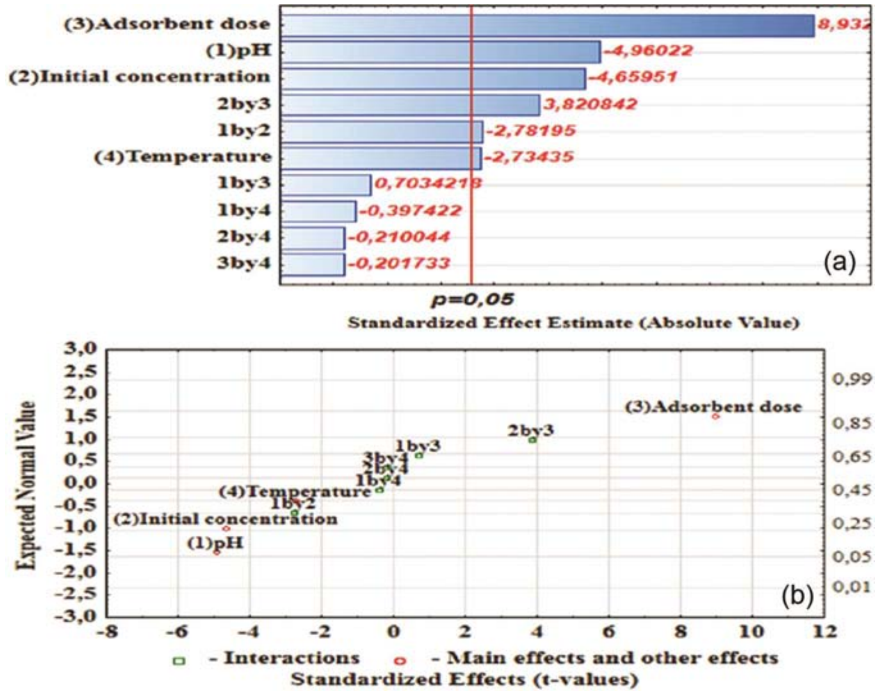

Fig. 5(a) — Normal probability plots of standardized effects of the studied factors and their interactions (b) Pareto chart of standardized effects

Table 8—Analysis of variance (ANNOVA) of the response surface quadratic model for phenol adsorption

Factors	Sun of Square	*df*	Mean Square	F value	P value
X_1	1077.481	1	1077.481	24.60377	0.004247
X2	950.797	1	950.797	21.71102	0.005535
X3	3493.992	1	3493.992	79.78370	0.000293
X4	327.429	1	327.429	7.47669	0.041067
X1X2	338.928	1	338.928	7.73927	0.038812
X1X3	21.669	1	21.669	0.49480	0.513189
X1X4	6.917	1	6.917	0.15794	0.707455
X2 X3	639.331	1	639.331	14.5988	0.012363
X2 X4	1.932	1	1.932	0.04412	0.841924
X3X4	1.782	1	1.782	0.04070	0.848076
Error	218.967	5	43.793		
Total SS	7079.225	15			
Standard error			2.64		

freedom and 16 factorial tests $F_{0.05,\ 1,\ 16}$ is equal to 4.49. All the effect with F-value higher than 4.49 and p value less than or equal to 0.05 are significant. By observing the F and p values from Table 8 it was observed that all main factors, X1X2 and X2X3 interactions effect were significant. The interaction effect X1X3, X1X4, X2X4 and X3X4 were not significant.

According to the student's test and F-test, the interaction effect X_1X_3, X_1X_4, X_2X_4 and X_3X_4 can be excluded from the regression equation. Then Eq 9 simplifies to Eq 10.

$$Y = 73.283 - 8.206X1 - 7.709X2 + 14.777X3 - 4.524X4 - 4.603X1X2 + 6.321X2X3 \quad \dots (10)$$

Based on Eq 10, the model was recalculated, eliminating the effect of insignificant factors. Table 9 showed the analysis of variance for the reduced model.

The coefficient of determination (R^2) and the adjusted determination coefficient values of this reduced model were recalculated as 0.96451 and 0.94084, respectively.

The observed and predicted removal efficiency plot for phenol was plotted. It was observed that the data

Table 9 — Analysis of variance reduced model fit (ANOVA)

Factors	Sun of Square	*df*	Mean Square	F value	P value
X_1	1077.481	1	1077.481	38.5937	0.000157
X2	950.797	1	950.797	34.0561	0.000248
X3	3493.992	1	3493.992	125.1496	0.000001
X4	327.429	1	327.429	11.7280	0.007572
X1X2	338.928	1	338.928	12.1399	0.006892
X2 X3	639.331	1	639.331	22.8999	0.000994
Error	251.267	9	27.919		
Total SS	7079.225	15			
Standard error		2.64			

points were well-distributed close to a straight line (R^2 = 0.9726), which suggested a good correlation between the observed and predicted values of the response, providing evidence for the validity of the regression model.

Effect of process variables on phenol removal

For the graphical interpretation of the interactions, use of 3D plots for the regression model is highly recommended[29]. Three-dimensional (3D) response surface plots as a function of two factors by keeping another factor at fixed level are the best way to identify the relation between the main and the interaction effects of these two factors.

Three dimensional (3D) response surface plots were used to determine adsorption for phenol over interactive variable. The surface plots were generated to investigate the effects of four process parameters, i.e. initial solution *p*H, initial phenol concentration, adsorbent dose and temperature on phenol removal. The influences of the four different process variables on the response factor are shown in the 3D response surface plots (Fig. 6).

Effect of *p*H

The adsorption of phenol from aqueous solution is dependent on the pH of the solution, which affects the surface charge of the adsorbent, degree of ionization, and speciation of the adsorbate species. Also, *p*H controls the electrostatic interactions between the adsorbent and adsorbate.

To elucidate the influence of *p*H on the phenol adsorption by granular activated carbon, the batch experiments were conducted with initial *p*H values ranging from 6.0 to 11.0. Figures 6a, b and c show the combined effect of initial *p*H with initial phenol concentration, temperature and absorbent dose based on the fitted first-order polynomial equation. The highest adsorption of phenol on this carbon occurred at the initial *p*H of the solution (pH_s=6), as observed by several workers[30-32]. Phenol is hydrophobic ionisable organic compound that can exist as the protonated species depending on the solution *p*H. The pK_a of phenol was found to be 9.9. Since the pH_{pzc} was found to be 7.2. GAC surface has positive charge when solution *p*H is less than pH_{pzc} and its negative if $pH > pH_{pzc}$. At *p*H 6 ($pH < pH_{pzc}$), the majority of phenol molecules are neutral or deprotonated, which can be easily adsorbed by the partially protonated chemical groups of GAC surface. At this *p*H the removal efficiency of phenol reached an ultimate value of 99.22% (run n.o.7)[33].

At *p*H> 6.0, the removal efficiency of phenol tends to decrease remarkably. Since at *p*H higher than 9.9 phenol molecules are in their dissociated and anionic forms, and the GAC surface is negatively charged. In this condition, the electrostatic repulsion between the surface and adsorbate reaches its maximum value; as a result the phenol will be adsorbed to a lesser extent[34,35]. At the same time, the presence of OH^- ions into the solution phase prevents the adsorption of phenolate ions[36,37]. Consequently, maximum removal efficiency reduced to 87.33% at *p*H 11.

Effect of initial phenol concentration

Phenol adsorption onto activated carbons was carried out at different initial phenol concentrations ranging from 50 to 1000 mg/L.

Figure 6a, d and e show the effect of initial phenol concentrations on adsorption while keeping one parameter constant. As seen from the results, the removal efficiency of phenol decreased gradually with increase in initial phenol concentration. This might be due to the decreased of available sites on the

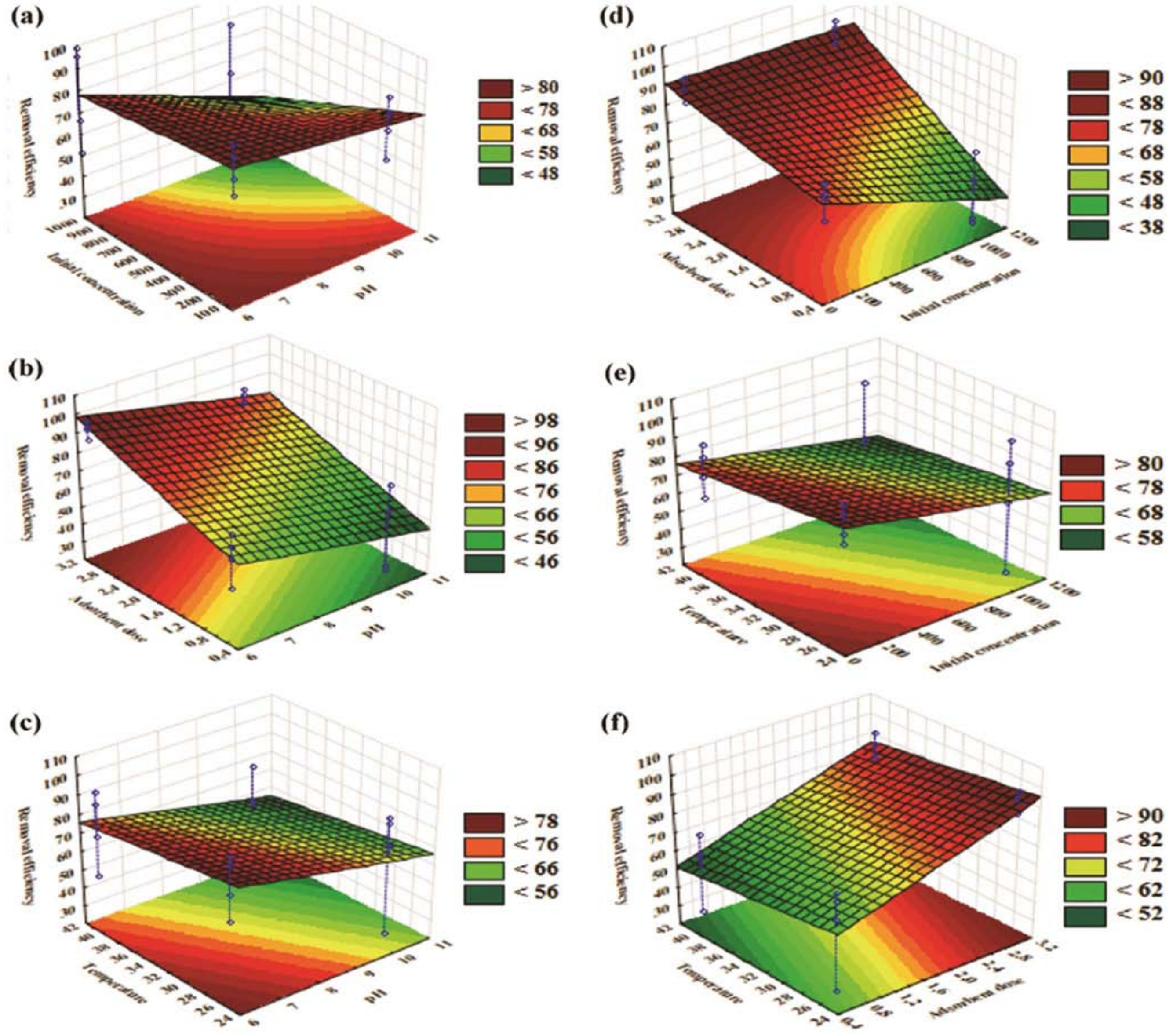

Fig. 6 — Response surfaces for the FFD: (a) initial concentration-*p*H; (b) adsorbent dose- *p*H;(c) temperature-*p*H; (d) adsorbent dose-initial concentration;(e) temperature- initial concentration;(f) temperature- adsorbent dose.

adsorbent surface at higher concentrations[38]. Under studied conditions, maximum removal efficiency was attained at an initial phenol concentration of 50 mg/L.

Effect of adsorbent dose

Based on the ANOVA results (Table 8), adsorbent dose had a greatest effect on phenol removal. The effect of the adsorbent dose was studied by varying the sorbent amounts from 0.5 to 3 g.

As shown in Figs 6b, d and f it was obvious that the removal efficiency of phenol increases from 28.57 to 87.33% when the adsorbent dose was increased from 0.5 to 3 g per 100 mL of solution. This trend might be due to greater availability of the surface area at higher mass of the adsorbent[39].

Effect of temperature

The adsorption experiments were performed in the temperature range of 25-40°C. The effect of temperature can be inferred from Figures 6c, e and f. The removal efficiency was found as 80.19% at 25°C (run no.1) where it decreased to 72.98% at 40°C (run no.9). This mainly due to the decrease in surface activity suggesting that adsorption between phenol and GAC is an exothermic process. This situation can be identified by thermodynamic parameters of adsorption such as standard enthalpy change (ΔH_T°), standard free energy (ΔG_T°) and standard entropy change (ΔS_T°). These parameters can be evaluated from the following Equation (Eqs 11-14):

$$K = \frac{C_{Ae}}{C_e} \quad \ldots (11)$$

$$\Delta G_{\mathrm{T}}^\circ = -RT \operatorname{Ln} K \quad \ldots (12)$$

$$\Delta G_{\mathrm{T}}^\circ = \Delta H_{\mathrm{T}}^\circ - \mathrm{T} \quad \ldots (13)$$

$$\mathrm{LnK} = \left(\frac{\Delta S_{\mathrm{T}}^\circ}{\mathrm{R}}\right) - \left(\frac{\Delta H_{\mathrm{T}}^\circ}{\mathrm{R}}\right) . \frac{1}{\mathrm{T}} \quad \ldots (14)$$

where K is the equilibrium constant, C_{Ae} (mg/L) and C_e (mg/L) indicates the phenol Equilibrium concentration on adsorbent phase and adsorbate phase, respectively. R is the universal gas constant (8.314 J/mol K), T is absolute temperature. The value of ΔS_T° and ΔH_T° are determined from the slope and intercept of plot Ln K versus 1/T. The ΔG_T° values were calculated using Equation 13. Thermodynamic data were given in Table 10. The standard Gibbs free energy values ΔG° were found to be negative, which indicated the feasibility and spontaneity of the adsorption. The negative value of the standard enthalpy change ΔH° confirmed the exothermic nature of adsorption process. The negative value of the standard entropy ΔS° reflects the decreased randomness at the solid solution interface during the adsorption process.

Optimization using the desirability functions

The desirability function approach is one of the most widely used methods for the optimization of multiple response processes. For each response, a desirability function assigns numbers between 0 and 1 to the possible values of response, with desirability function equal to 0 representing a completely undesirable value of response and desirability function equal to 1 representing a completely desirable or ideal response value. The profile for predicted values and desirability in the STATISTICA 12 software is used for the optimization process. The desirability of 1.0 was assigned for the maximum removal (99.22%), 0.0 for the minimum (28.57%) and 0.5 for the middle (63.89%). The desirability function was used to find combination of levels of process parameters that produce the maximum desirable response. Also the desirability score of 1.0, maximum recovery (99.22%) was obtained in optimum conditions set as: *p*H 6, the initial phenol concentration of 1000 mg/L, 3g of adsorbent at a temperature of 28.75°C.

Table 10—Thermodynamic data for adsorption of phenol

Temperature (K)	ΔG° (KJ/mol)	ΔH° (kJ /mol)	ΔS° (KJ/mol K)
289	-10,258		
298	-9,146	-45,943	-0,123
313	-7,294		

Adsorption isotherms

In order to obtain adsorption isotherms, equilibrium adsorption experiments were carried with different phenol concentrations at three temperatures (289, 298 and 313 K). Equilibrium data which was commonly known as adsorption isotherms indicate how the adsorption molecules distribute between the liquid phase and the solid phase in the whole adsorption process, and give a comprehensive understanding of the nature of adsorption. The equilibrium data obtained from different models provides important information on the properties of the adsorbent surface. In this study, five isotherm models (Langmuir, Freundlich, Temkin, Dubinin-Radushekevich (D-R), Redlich-Peterson) were applied to describe the Equilibrium characteristics of adsorption.

Langmuir isotherm

The Langmuir isotherm[40] is based on the assumption that adsorption takes place at specific homogeneous sites within the adsorbent and once a phenol molecule occupies a site, no further adsorption takes place at that site. The Langmuir isotherm Equation is given as:

$$\mathrm{q_e} = \frac{\mathrm{q_m K_L C_e}}{1 + \mathrm{K_L C_e}} \quad \ldots (15)$$

where C_e is the concentration of the phenol solution (mg/L) at equilibrium, q_e is the amount of adsorbate adsorbed per unit mass of adsorbent at equilibrium (mg/g), q_m and K_L are the Langmuir constants related to adsorption capacity (mg/g) and free energy of adsorption (L/mg), respectively.

In order to determine if the adsorption process is favorable or unfavourable, a dimensionless constant separation factor or equilibrium parameter R_L, is defined according to the following equation[41]:

$$\mathrm{R_L} = \frac{1}{1 + \mathrm{K_L C_0}} \quad \ldots (16)$$

where K_L is the Langmuir constant (L/mg) and C_0 is the initial phenol concentration (mg/L). The value of

R_L indicates the type of isotherm to be favourable ($0<R_L<1$), linear ($R_L=1$), unfavourable ($R_L>1$), or irreversible $R_L=0$.

Freundlich isotherm

The Freundlich isotherm is an empirical equation assuming that the adsorption process takes place on a heterogeneous surface through a multilayer adsorption mechanism, stronger binding sites are occupied first and that the binding strength is related to the concentration of phenol at equilibrium[42]. The Freundlich equation can be given by the equation:

$$q_e = K_F C_e^{1/n} \qquad \ldots (17)$$

where K_F (L/mg) and n are indicators of adsorption capacity and adsorption intensity, respectively.

Temkin isotherm

The Temkin isotherm[43] takes the effects of indirect adsorbate–adsorbate interactions on adsorption into account, and suggests that because of these interactions the heat of adsorption of all the molecules in the layer would decrease linearly with coverage. The Temkin isotherm is expressed as:

$$q_e = B \ln(A C_e) \qquad \ldots (18)$$

where B (J/mol) = RT/b_T is the Temkin constant which is related to the heat of adsorption while A (L/mg) is the equilibrium binding constant. R (8.314 J/mol K) is the universal gas constant and T (K) is the absolute solution temperature.

Dubinin-Radushklevich

Dubinin-Radushklevich isotherm is applied to find out the adsorption mechanism based on the potential theory assuming heterogenous surface[44].

The Dubinin-Radushkevich adsorption isotherm is expressed as:

$$q_e = q_D \exp(-K_D \varepsilon^2) \qquad \ldots (19)$$

where q_D is the theoretical monolayer saturation capacity (mg/g), K_D is the Dubinin–Radushkevich model constant (mol^2/kJ^2) and ε is the Polanyi potential and is equal to:

$$\varepsilon = \mathrm{RT\,Ln}\left(1 + \frac{1}{C_e}\right) \qquad \ldots (20)$$

R (8.314 J/mol/K) is the universal gas constant and T (K) is the absolute solution temperature.

The constants K_D (mol^2/kJ^2) approach was usually applied to distinguish the physical and chemical adsorption of metal ions with its mean free energy[45]. The adsorption energy, E, can be calculated as follows:

$$E = \frac{1}{\sqrt{2K_D}} \qquad \ldots (21)$$

Redlich-Peterson

Redlich and Peterson[46] incorporated three parameters into an empirical isotherm. The Redlich–Peterson equation is used as a compromise between Langmuir and Freundlich, and the mechanism of adsorption is a hybrid unique and does not follow ideal monolayer adsorption. It can be described as follows:

$$q_e = \frac{K_{RP} C_e}{1 + \alpha_{RP} C_e^{\beta}} \qquad \ldots (22)$$

where K_{RP} (L/mg) and α_{RP} (L/mg) are the Redlich-Peterson isotherm constants, while β is the exponent, which lies between 0 and 1.

The various isotherms obtained were analyzed by non-linear regression analysis using Origin Pro 8.6 software. The sum of squares due to the errors (SSE) and the average relative error (ARE) of the obtained models are calculated so as to evaluate the goodness of fit. Also the compatibility between experimental and theoretical isotherm data was checked with correlation coefficients (R^2).

These error functions employed are as follow:

(i) The sum of the square of the errors (SSE)

$$\sum_{i=1}^{n} \left(q_{e,cal} - q_{e,exp}\right)^2 \qquad \ldots (23)$$

where n is number of data points, $q_{e,exp}$ is amount of adsorbate adsorbed at equilibrium obtained from experiment (mg/g) and $q_{e,calc}$ is amount of adsorbate adsorbed at equilibrium obtained from the models (mg/g).

(ii) The average relative error (ARE)

$$\backslash\sum_{i=1}^{n} \frac{|q_{e,exp} - q_{e,cal}|}{q_{e,exp}} \times \frac{100}{n} \qquad \ldots (24)$$

The fitted parameter values and the determined error function values are listed in Table 11. The results indicated that both the Redlich–Peterson and the Freundlich isotherms had almost the same coefficients of determination were greater than 0.99 at all three temperatures studied (Table 11). In addition the Redlich–Peterson and Freundlich isotherms seemed to be the best-fitting models for the experiment results from Fig. 7. At all studied temperature the Redlich–Peterson and Freundlich isotherms had coefficients of determination (R^2) higher than the case of Langmuir which indicated that the Redlich–Peterson isotherm was approaching the Freundlich form but not the Langmuir isotherm. Consequently, the adsorption of phenol on the activated carbon was best described by the Redlich–Peterson and Freundlich isotherms basing on the highest R^2 value and the lowest (SSE) and (ARE) values. The K_F value shows a decrease tendency with the rise of temperature, and the n values lie mostly in the range of 1-10, indicating favorable adsorption of phenol GAC at studied conditions. The Langmuir maximum adsorption capacity Qmax for phenol adsorption onto granular activated carbon decreased from 317.675 to 276.231 mg/g with the increase in temperature from 289 to 313K. As shown in Table 12, the calculated R_L values were between 0 and 1, indicating that the adsorption of phenol on the activated carbon was favorable in this study and as the initial concentration increased the values of R_L decreased which showed that the adsorption was more favorable at higher initial concentration. For the Dubinin-Radushkevich model, their equation represents the poorer fit of the experimental data than the others isotherm equations. The magnitude of the adsorption energy, E, was found to be in the range of 3.012-4.442 kJ /mol, which is less than 8 kJ /mol, suggested that the adsorption reactions is physical. Comparing the correlation coefficient, it is clear that Freundlich isotherm best fits the experimental data at higher temperature but at lower temperatures, Redlich–Peterson isotherm best fits the data, indicating the heterogeneity of the sorbent surface.

Adsorption kinetic models

The effect of contact time on adsorption rate was investigated to find equilibrium time for adsorption. A plot of amount of phenol adsorption in various contact time with different C_0 (10- 500 mg/L) was plotted. The rate of phenol removal is found to be very rapid during the initial 30 min and thereafter the rate of phenol removal decreases. No significant change in phenol removal is observed after about 120 min. Also equilibrium time was obtained after about 120 min.

Table 11—Isotherm parameters for the adsorption of phenol by GAC

Isotherm	Parameters	Temperature (K) 289	298	313
Langmuir	K_L (L/mg)	0.0067	0.0053	0.0035
	q_m(mg/g)	317.675	305.964	276.231
	R^2	0.9317	0.9379	0.8717
	SSE	3128.49	1871.87	3887.89
	ARE	40.53	32.43	44.81
Freundlich	K_F (L/mg)	23.700	16.845	13.406
	n	2.745	2.496	2.478
	R^2	0.9910	0.9931	0.9682
	SSE	411.29	277.02	961.34
	ARE	24.60	24.60	21.17
Temkin	B (J/mol)	37.980	30.933	27.134
	A (L/mg)	2.748	1.028	0.892
	R^2	0.8907	0.8990	0.8587
	SSE	16395.81	5418.95	4666.69
	ARE	69.05	33.93	22.35
Dubinin-Raduskevich	q_D (mg/g)	180.742	175.809	152.680
	K_D (mol^2/KJ^2)	5.509E-02	3.528E-02	2.533E-02
	E (KJ/mol)	3.012	3.764	4.442
	R^2	0.5867	0.6152	0.5854
	SSE	18930.41	15480.95	12631.03
	ARE	51.21	53.23	49.02
Redlich-Peterson	K_R (L/mg)	273.725	35.306	21.106
	α_R (L/mg)	11.161	1.816	1.077
	β	0.640	0.619	0.656
	R^2	0.9911	0.9939	0.9655
	SSE	406.36	247.12	1203.96
	ARE	22.36	17.75	17.02

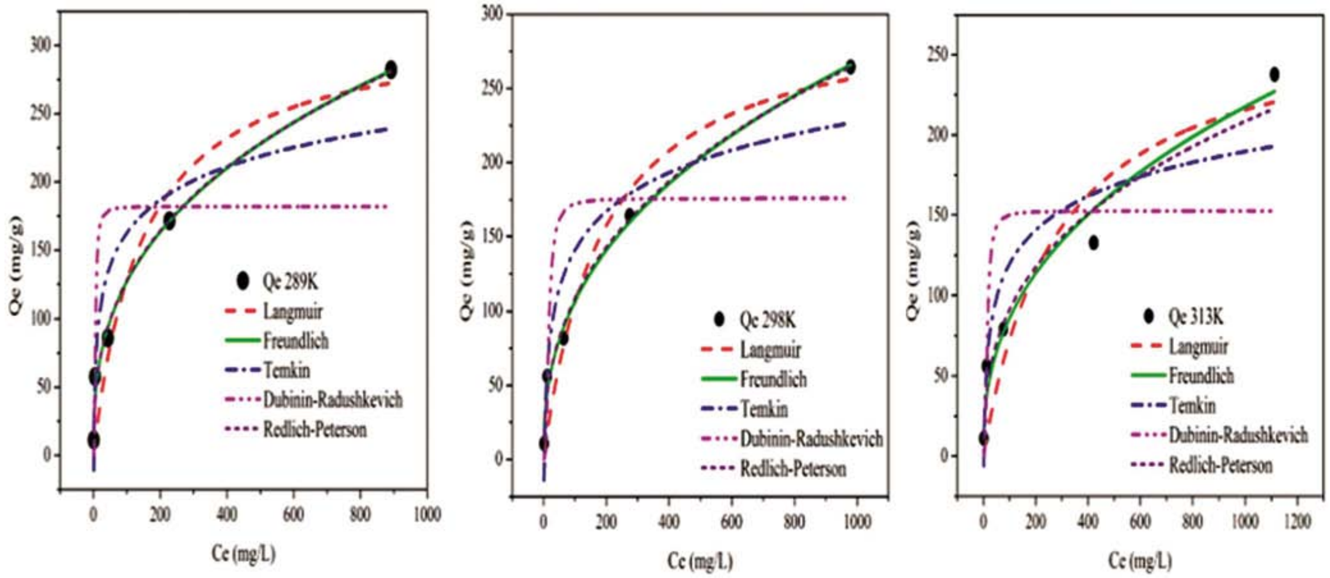

Fig. 7 — Comparison of different isotherm models for phenol adsorption on GAC.

Table 12—Dimensionless separation factor (R_L) values for phenol adsorption by GAC

Phenol concentration (mg/L)	R_L		
	289K	298K	313K
50	0.5245	0.6219	0.6901
250	0.1807	0.2476	0.3081
500	0.0993	0.1413	0.1821
1000	0.0523	0.0760	0.1002
2000	0.0268	0.0395	0.0527

The adsorption kinetics describes the efficiency and the rate of the process and it controls the equilibrium time. In order to investigate the rate and the mechanism of adsorption of phenol on this activated carbon, the pseudo-first-order and the pseudo-second-order kinetic models were studied and then the intraparticle diffusion model was further tested to determine the diffusion mechanism.

The pseudo-first-order Equation given by Langergren and Svenska[47] can be expressed as:

$$q_t = q_e\left(1 - exp(-K_1 t)\right) \quad \ldots (25)$$

where q_e and q_t are the amounts of phenol adsorbed at equilibrium and at time t in mg/g, respectively, and K_1 is the pseudo-first-order rate constant (1/min).

The pseudo-second-order kinetic model can be given in the following form[48]:

$$q_t = \frac{K_2 q_e^2 t}{1+K_2 q_e t} \quad \ldots (26)$$

where K_2 is the rate constant of pseudo-second-order adsorption (g/mg min).

As the above kinetic models were not able to identify the diffusion mechanisms and rate controlling steps in the adsorption process, the intraparticle diffusion model based on the theory proposed by Weber and Morris[49] was tested. According to this theory, the intraparticle diffusion Equation can be expressed as:

$$q_t = K_{dif} t^{1/2} + C \quad \ldots (27)$$

where K_{dif} (mg/g $min^{0.5}$) is the intraparticle diffusion rate constant and C is the intercept, gives an idea about the thickness of boundary layer. If the plot of adsorption capacity, qt versus $t^{1/2}$ is a straight line (C=0), the intra particle diffusion is involved. Moreover, if the line passes through the origin, diffusion in the sorbent is the only controlling step. Otherwise, some other mechanism along with intraparticle diffusion is also involved.

The various kinetic model used to describe the adsorption process were analyzed by non-linear regression analysis using OriginPro8.6 software and was verified through the correlation coefficients (R^2), the sum of squares due to the errors (SSE) and the average relative error (ARE).

Figure 8 illustrates the kinetic models that are fitted to the experimental data. Kinetic parameters along with correlation coefficient and error function obtained from various graphical presentations of kinetic equations are listed in Table 13.

The correlation coefficients were found higher for pseudo-first-order kinetic model than the pseudo-

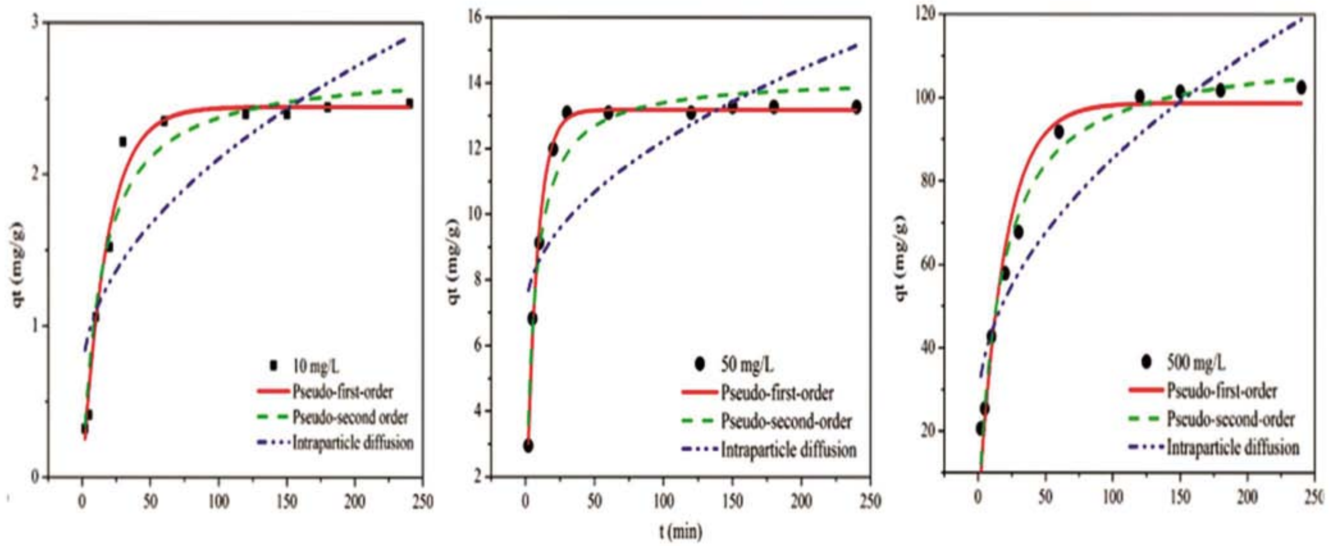

Fig. 8 — Comparison of different kinetic models for phenol adsorption on GAC.

Table 13—Kinetic parameters for the adsorption of phenol by GAC

Model	Parameters	Concentrations (mg/L)		
		10	50	500
First- order kinetic	K_1(1/min)	0.055	0.128	0.052
	q_e(mg/g)	2.443	13.184	98.726
	R^2	0.9840	0.9947	0.9551
	SSE	0.108	0.611	312.803
	ARE	8.793	2.027	10.938
Second-order kinetic	K_2(g/mg min)	0.026	0.019	5.395E-04
	q_e(mg/g)	2.707	14.192	111.767
	R^2	0.9589	0.9801	0.9866
	SSE	0.277	9.342	52780.654
	ARE	11.742	12.683	95.120
Intraparticle diffusion	K_{dif} (mg/g min $^{0.5}$)	0.146	0.530	6.081
	C	0.634	6.928	24.628
	R^2	0.7325	0.5617	0.8732
	SSE	1.805	50.543	1234.280
	ARE	40.246	27.160	19.228

second-order kinetic model, indicating excellent applicability of the pseudo-first-order kinetic model to describe the adsorption process of phenol on GAC. Error functions as shown in Table 13 are also considerably less for pseudo-first-order kinetic model reinforcing the applicability of the pseudo-first-order kinetic model. In addition, the values experimental q_e (2.396, 13.087, 100.276 mg/g) were found to be close to the calculated data (2.443, 13.184, 98.726 mg/g) at different initial concentrations, which also shows good agreement. For intraparticle diffusion, the values of correlation coefficients are much lower than the other kinetic values. In all cases, their Equation represents the poorer fit of experimental data than the other kinetic models. From the Table 13 the value of intercept (C) was higher than zero, so the regression was not linear for all concentrations. This result suggests that in addition to intraparticle diffusion the first order kinetic model is involved in the phenol adsorption.

Effect of ionic strength

Phenol removal might be affected by the presence of dissolved salts in the aqueous solutions, so the effect of salinity on the adsorption of phenol was also studied. Solutions containing 50 mg/L of phenol concentration were tested after addition of either sodium chloride (NaCl) or calcium chloride ($CaCl_2$) or sodium sulfate (Na_2SO_4). Figure 9 shows the effect of various concentrations (0, 0.0001, 0.001, 0.01, 0.1 M) of electrolytes on the percentage removal of phenol. It is found that the percentage removal of phenol

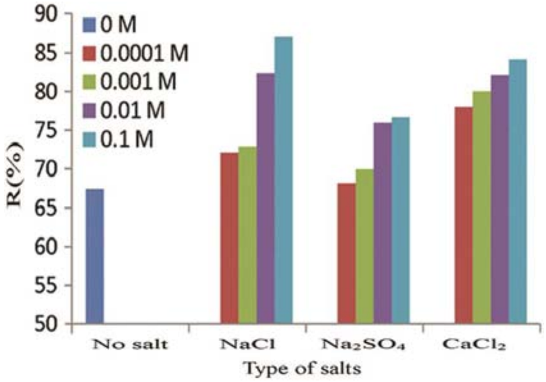

Fig. 9 — Effect of ionic strength.

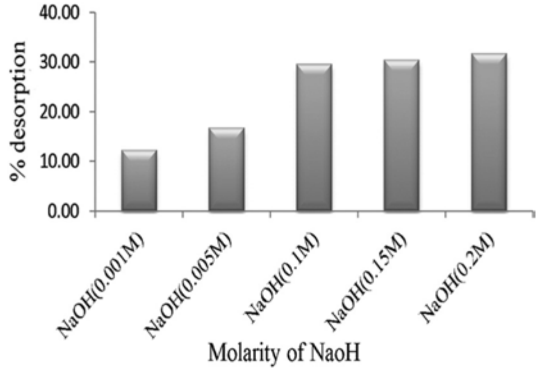

Fig. 10 — Desorption of phenol with different concentrations of NaOH.

Table 14 — Comparison of the maximum monolayer adsorption of phenol onto various adsorbents

Adsorbent	Adsorbate	Adsorption capacity (mg g^{-1})	pH	Contact time (hours)	References
Bentonite	Phenol	66.67	6	1	[48]
Powdered F400 carbon	Phenol	83.33	6	1	[48]
Bagasse fly ash	Phenol	23.33	6	2	[16]
Graphene	Phenol	49.51	6.3	48	[49]
Zeolite Y (HFAU)	Phenol	13.61	6	1	[50]
GAC (NORIT 1240W)	Phenol	294.11	6	2	This study

increased with the concentrations of electrolyte. These results are explained through the addition of electrolyte to the solution which can cause a salting-out effect. The salting-out is an effect based on the electrolyte-non electrolyte (i.e. phenol) interaction, in which the non-electrolyte could be less soluble at high salt concentrations. When the salt concentration is increased, some of the water molecules are attracted by the salt ions, which decreases the number of water molecules available to interact with organic solute. This phenomenon will reduce the solubility of a phenol in water and thus intensify their diffusion process into the carbon surface[15].

Desorption studies

Desorption studies help to elucidate the mechanism of adsorption as to recover the pollutants from the spent adsorbent apart from protecting the environment from solid waste disposal problem. Desorption of phenol was tried with 0.001, 0.005, 0.1, 0.15 and 0.2 M sodium hydroxide solutions. It was found that maximum desorption occurs in the case of 0.1 M NaOH solution (Fig. 10). The phenols react with NaOH to form sodium phenates which are readily desorbed. The adsorption of phenols on to the activated carbon is reversible. The spent adsorbent can be regenerated and reused upon treatment with 0.1 M NaOH.

Comparative study

Table 14 gives a comparison of the maximum monolayer adsorption of phenol onto various adsorbents obtained from adsorption experiments. The granular activated carbon (GAC) used in this study had a high adsorption capacity of 294.11 mg/g compared to some other adsorbents reported in the literature.

Conclusion

Phenol adsorptive properties of granular activated carbon (GAC) have been systematically studied. The GAC has been characterized using different technique such as SEM, BET, FTIR and XRD. The process parameters (*p*H, adsorbent dose, initial concentration and temperature) were optimized using FFD combined with RSM. Based on the FFD, the linear mathematical model representing the influence of different variable and their interaction was developed. Analysis of variance, suggested that the predicted values were in good agreement with experimental data and the adsorbent dose was the most significant factor affecting phenol removal. The optimum conditions were determined by applying the method of desirability function. Batch adsorption experiments indicate that the adsorption equilibrium can be achieved within 120 min. The adsorption of phenol onto granular activated carbon is best fitted by a pseudo first order kinetic model. Experimental data were analyzed using Langmuir, Freundlich, Dubinin–Radushkevich, Temkin, Redlich-Peterson isotherm models and it was found that the Freundlich and Redlich-Peterson model presented a better fit. FTIR spectrum confirmed the presence of phenol on the GAC surface. The calculated thermodynamic parameters indicated the feasibility, exothermic and spontaneous nature of the adsorption process. The spent adsorbent can be regenerated by alkali treatment.

References

1 Venkateswaran P & Palanivelu K, *J Hazard Mater*, 131 (2006) 146.

2 Abdelwahab O, Amin N K & El-Ashtoukhy E Z, *J Hazard Mater*, 163 (2009) 711.

3 Bayramoğlu G & Arıca M Y, *J Hazard Mater*, 156 (2008)148.

4 Tepe O & Dursun A Y, *J Hazard Mater*, 151 (2008) 9.

5 (ATSDR) Agency for Toxic Substances & Disease Registry, *Toxicological Profile for Phenol*, US Department of Health & Human Services, Public Health Service, Atlanta, GA (1998).

6 (WHO) World Health Organization. *Health Criteria & Supporting Information*, WHO Guidelines for Drinking Water Quality, (vol. II), Geneva, Switzerland (1984).

7 Dutta N N, Borthakur S & Baruah R A, *Water Environ Res*, 70 (1998) 4.

8 Dursun G, Cicek H & Dursun A Y, *J Hazard Mater*, 125 (2005) 175.

9 Y M Awad & N S Abuzaid, *Sep Purif Technol*, 18 (2000) 227.

10 Das A & Sharma D K, *Energy sources*, 20 (1998) 821.

11 Reis M T A , de Freitas O M , Ismael M R C & Carvalho J M, *J Membr Sci*, 305 (2007) 313.

12 Tabassi D, Mnif A & Hamrouni B, *Desalin Water Treat*, 52 (2014) 1792.

13 Bertoncini C, J.Raffaelli J, Fassino L, Odetti H S, & Bottani E J, *Carbon*, 41(2003) 1101.

14 Radovic L R, Moreno-Castilla C & Rivera-Utrilla J, *Chem Phys Carbon*, (2001) 227.

15 Lazo-Cannata J C, Nieto-Márquez A, Jacoby A, Paredes-Doig A L, Romero A, Sun-Kou M R & Valverde J L, *Sep Purif Technol*, 80 (2011) 217.

16 C.Srivastava V, Swamy M M, Mall I D, Prasad B & Mishra I M, *Colloids Surf A*, 272 (2006) 89.

17 Box G E & Wilson K B, *J R Stat Soc Ser B Stat Methodol*, 13 (1951) 1.

18 Montgomery D C & Wiley J, (John Wiley & Sons, New York), 2001.

19 Gottipati R & Mishra S, *Chem Eng J*, 160 (2010) 99.

20 Bingol D, Tekin N & Alkan M, *Appl Clay Sci*, 50 (2010) 315.

21 Barrett E P, Joyner L G & Halenda P P, *J Am chem Soc*, 73 (1951) 373.

22 Boehm H P, *Carbon,* 32 (1994) 759.

23 M.Babić B, Milonjić S K, Polovina M J & V Kaludierović B, *Carbon,* 37 (1999) 477.

24 Rodier J L, *Analyse chimique et physico chimique de l'eau*, 9th Edn, (2009).

25 Mastalerz M & Bustin R M, *Fuel,* 74 536 (1995).

26 Rameshraja D, Srivastava V C, Kushwaha J P & Mall I D, *Chem Eng J*, 181 (2012) 343.

27 Suresh S, Srivastava V C & Mishra I M, *Sep Sci Technol*, 46 (2011) 1750.

28 IUPAC, Manual of Symbols and Terminology of Colloid Surface, Butterworths, London, (1982).

29 Aktaş N, *Enzyme Microb Technol*, 37 (2005) 441.

30 El-Naas M H, Al-Zuhair S & Alhaija M A, *Chem Eng J*, 162 (2010) 997.

31 Kilic M, Apaydin-Varol E & Pütün A E, *J Hazard Mater*, 189 (2011) 397.

32 Rodrigues L A, da Silva M L C P, Alvarez-Mendes M O, dos Reis Coutinho A & Thim G P, *Chem Eng J*, 174 (2011) 49.

33 Liu Q S, Zheng T, Wang P, P Jiang J & Li N, *Chem Eng J*, 157 (2010) 348.

34 Banat F A, Al-Bashir B, Al-Asheh S & Hayajneh O, *Environ Pollut*, 107 (2000) 391.

35 Khalid N, Ahmad S, Toheed A & Ahmed J, *Appl Radiat Isot*, 52 (2000) 31.

36 Rengaraj S, Moon S H, Sivabalan R, Arabindoo B & Murugesan V, *Waste Manage*, 22 (2002) 543.

37 Nath K, Thummar M, Vaghela M & Jani P, *Indian J Chem Technol*, 15 (2008) 533.

38 Kilic M, Apaydin-Varol E & Pütün A E, *J Hazard Mater*, 189 (2011) 397.

39 Langmuir I, *J Am Chem Soc*, 37 (1915) 1139.

40 Weber T W & Chakravorti R K, *AIChE J*, 20 (1974) 228.

41 Freundlich H M F, *J Phys Chem*, 57 (1906) 385.

42 Temkin M I & Pyzhev V, *Acta Physiochim*, 12(1940) 217.

43 Do D D, *World Scientific*, (1998).

44 Dada A O, Olalekan A P, Olatunya A M & Dada O, *J Appl Chem*, 3 (2012) 38.

45 Redlich O & Peterson D L, *J Phys Chem*, 63 (1959) 1024.

46 Lagergren S, *K Sven Vetenskapsakad H&l*, 24 (1898) 1.

47 Ho Y S & McKay G, *Process Biochem*, 34 (1999) 451.

48 Özacar M & Şengil İ A, *Process Biochem*, 40 (2005) 565.

49 Hank D , Azi Z , Hocine S A, Chaalal O & Hellal A , *J Ind Eng Chem*, 20 (2014) 2256.

50 Li Y , Du Q , Liu T, Sun J , Jiao Y, Xia Y & Wu D, *Mater Res Bull*, 47 (2012) 1898.

51 Chaouati N, Soualah A & Chater M, *C R Chim*, 16 (2013) 222.